
# UNIVERSITÀ DEGLI STUDI DI PADOVA

**Dipartimento di Fisica e Astronomia "Galileo Galilei"**

**Corso di Laurea in Fisica**


**Tesi di Laurea**

# Dosimetric evaluation of radiopharmaceuticals containing Mn radioisotopes


**Relatore**

**Prof.ssa Laura de Nardo**

**Correlatore**

**Dr.ssa Laura Melèndez-Alafort**

**Laurendo**

**Michele Morella**


**Anno Accademico 2017/2018**

# Contents

# Introduction

Radiopharmaceuticals, also known as radiotracer, are molecules labelled with radioactive nuclides used to study the insight of the human body noninvasively and *in vivo*; this means that we are able to have a look at what's happening inside patient's body at molecular level using appropriate diagnostic techniques, such as PET (Positron Emission Tomography). In the era of personalized medicine, radiopharmaceuticals are a powerful tool even for therapy [2].

Goal of this work is to try to assess the amount of radiation that a human would absorb by exposure to $^{51}Mn$ and $^{52}Mn$ starting from animal data taken from [4] and [19], both of them employing $MnCl_2$ as radiopharmaceutical. Although using $Mn$ in its ionic form hasn't very good biodistribution properties and shows some side-effects [9], many studies are conducted exploiting it and gathered data on it since it's the easiest manganese-based radiopharmaceutical to produce; yet, there are no dosimetric evaluation found in literature. In particular, $^{52}Mn$ is a long-lived isotope ($t_{1/2} = 5.591\,days$) thought to be employed in order to study biological processes and molecules with slow biodistribution (such as antibodies). It has been chosen because it is the only radionuclide with $1 < Z < 92$ having positron-emitting nuclear properties that resemble a lot those of $^{18}F$ (so that it can be employed as radiotracer for PET imaging) and it has very useful paramagnetic properties that makes it suitable to be used as MRI contrast agent. As a matter of fact there are experiments [12] [9] that shows both pros and cons of this metal, focusing their attention on the quality of the image it can produce in a possible MultiModal Imaging approach in diagnostic Nuclear Medicine that combines both PET/MRI; in this way it is possible using different diagnostic informations, improving the understanding of clinical conditions. A dosimetric assessment of these isotopes is important also because of the upcoming research project METRICS (*Multimodal pET/mRi Imaging with Cyclotron-produced* $^{52/51}Mn$ *and stable paramagnetic* $Mn$ *iSotopes*) that will take place also at INFN Legnaro National Laboratory that aims at produce as pure as possible $^{52}Mn$ through different possible reactions.

In the first chapter basic physical properties of these isotopes are presented and subsequently, after a brief introduction about the working principles of the two imaging modality that are going to exploit $^{51}Mn$ and $^{52}Mn$, their use as radiopharmaceuticals (and side effects) will be discussed. Afterwards, in third chapter, basic concepts of dosimetry will be introduced in order to apply them to data gathered in literature and evaluate the energy released by the radiation within the human body.

# Chapter 1

# $Mn$ radioisotopes physical properties

The $Mn$ isotopes that are going to be discussed and analyzed in the thesis are $^{52}Mn$ and $^{51}Mn$; in this chapter physical aspects and properties of this two radionuclides will be presented.

## 1.1 Decay scheme, positron energy and range

The $^{52}Mn$ decay to stable $^{52}Cr$ by electron capture (70.4%) and positron emission (29.6%) and has an half-life of 5.591 days. In order to perform dosimetric evaluations of the $Mn$ isotopes it is necessary to know how much energy would be released by the emitted positron in the decay reaction and how much lenght it would travel in the body before it annihilates with an electron. As for the energy, from Fermi's $\beta^+$ decay theory we know that this is a 3-body process so the positron energy is not completely determined from the masses of the particles involved in the decay (in the center of mass reference system); this means that in practice it's helpful to consider its possible maximum energy (when $\nu_e$ is produced at rest) known as *End point* energy or *Q-value* that is $Q = 575.5\,keV$. Sometimes even emitted positron mean energy can be taken in account $E_{mean} = 244.6keV$ [1] [3].

An important physical quantity to asses the distance traveled by a given particle in a medium is the *range* $R$ that is defined as the length that it covers until it stops

$$R = \int_0^{E_{tot}} \left(\frac{dE}{dx}\right)^{-1} dE$$

where $\frac{dE}{dx}$ is the energy loss per unit of length. This value gives information about the intrinsic loss of spatial resolution that is achievable in Nuclear Medicine imaging techniques like PET that exploit $e^+e^-$ annihilation to detect the radiopharmaceutical.

Although $^{52}Mn$ gamma emission scheme is pretty complicated (19 possible different emissions allowed) there are only three photons with high relative intensity that can be detected easily and they are showed in Figure 1.1; they are emitted in coincidence with the positron and they are $\gamma_1 = 744\,keV(90.0\,\%)$, $\gamma_2 = 936\,keV(94.5\,\%)$ and $\gamma_3 = 1434\,keV(100.0\,\%)$. Positron emitter nuclei are important for the use of $511\,keV$ annihilation $\gamma$s for PET scans and because of the emissions of previous high energy photons, it would be better to select a narrow window in the detector acquisition system in order to not reveal them. Actually some of these photons could be detected anyway because they could scatter inside the patient's body or inside the detector creating new photons with an energy that fits the restricted window of acceptance, producing false events. Also, these photons increases the energy absorbed by the body when using $^{52}Mn$-based radiopharmaceuticals.

The other nuclide that will be analyzed farther is $^{51}Mn$ ($t_{1/2} = 46.2\,min$, $E_{mean} = 970.2keV$ ) that decay $\beta^+$ to unstable $^{51}Cr$ with a probability of 97.1 %. Even though there are no prominent gamma emissions ($> 1\%$), additional dose contribution comes from the daughter nucleus $^{51}Cr$ that emits a $320\,keV$ gamma ray in 10% of the decays [4].

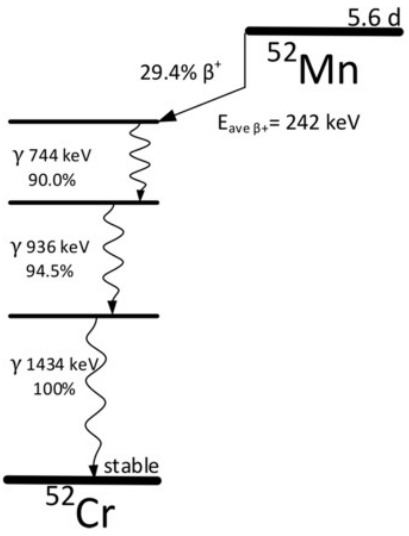


Figure 1.1: Simplified decay scheme of $^{52}Mn$ with only relevant gamma rays
The three $\gamma$s are emitted nearly in coincidence with the positron

## 1.2 Production

As for the production of the two $Mn$ isotopes there are some basic common procedures: first of all it's necessary to study the nuclear reactions with highest cross section and lowest amount of isotopic impurities (that cannot be eliminated by chemical separation) and then to find a chemical technique that allows to separate the requested nuclide from all the other elements produced in the target. The search for a good separation method must take in account the radioactive half-life of the radioisotopes since it could be quite small (e.g. $t_{1/2} = 46.2\,min$ for $^{51}Mn$) and this could lead to a low final yield of the product.

$^{52}Mn$ can be produced through different nuclear reactions:

- $^{51}V(^3He,t)\,^{52}Mn$ via this one a large quantity of impurities are produced (i.e.$^{49}V$, $^{51}Cr$ $^{52}Cr$) that actually can be easily removed from the sample with chemichal techniques [1];
- $^{nat}Cr(^3He,t)\,^{52}Mn$ that yet produces a remarkable amount of $^{53}Mn$ and thanks to its very long half-life ($\sim 10^6 years$) this reaction has not been investigated farther [1];
- $^{52}Cr(p,n)\,^{52}Mn$ is suitable for production in small cyclotrons although in this reaction it is often used $^{nat}Cr$ because of the high abundance of $^{52}Cr$ (83.7%); the use of natural chromium could be favorable for its lower cost than pure $^{52}Cr$ target even though there is a slight decrease of the cross section and the production of other isotopic contaminats ($^{51}Mn$, $^{52m}Mn$). [1]

Still there are more possible reactions (e. g. $^{52}Cr(d,2n)\,^{52m/g}Mn$) that can be employed, but the fundamental requirements are high cross section and radionuclidic purity, in order not to have contaminations that could limit the use of $^{52}Mn$ as radiopharmaceutical.

# Chapter 2

# Medical application: $Mn$-based radiopharmaceuticals

Radiopharmaceuticals are radioactive molecular probes that point out specific biological structures (cell receptors, proteins, enzymes) in order to detect their presence and distribution throughout the body of the subject being studied or destroy selected target by using radiation emitting nuclei (this radiation could be alpha particles or high energy positrons) . As for diagnostic application of radiopharmaceutical it's useful the definition given by the Society of Nuclear Medicine: "Diagnostic radiopharmaceuticals are substances that contain radionuclides that emit penetring radiations. [...] Dynamic and static images of the distribution of the radiopharmaceutical within the body can be obtained using a gamma camera or other suitable instrument appropriate for the radiopharamceutical being imaged, e.g. positron-emitting radiopharmaceutical" [6]. As well as radiopharmaceutical, molecular probes can be anything that once injected into the body and linked to an appropriate molecule can give information about its position by creating (under certain conditions) a signal detectable from the outside: this is the case, for examples, of paramagnetic metals used as contrast media to improve imaging with Magnetic Resonance technique in order to have a better contrast between selected tissues and the surrounding ones. This means that in general this molecular probes are made with the same basic entities: a structure that enables the probes to interact *in vivo* with the organism [1] and the signalling part that allows the revelation from outside. A schematic picture of this mechanism is shown in Figure 2.1, where it is possible to see that a linker is needed to connect the previous components.

## 2.1 PET and MRI imaging overview

Up to now we've seen what a radiopharmaceutical, or more generally speaking a molecular probe, is and how we can use it to gain informations for diagnostic purpose. Obviously different nuclei (positron emitting or paramagnetic ones) need different tools to be detected in the laboratory: these are PET and MRI that are techniques widely used all over the world in daily diagnosis routine and the developement of better instrumentation and improvement passes also through the search for new elements to be used. These elements will be later exploited as radiotracer because of their particular type of radiation emitted, as contrast media because of their paramagnetic properties or even both simultaneously: one of the reasons why $^{51}Mn$ and $^{52}Mn$ have been studied in the last decades is that they show very good properties in possible applications for a joint PET/MRI imaging tool. Basic working principles of the detecting part and the different physical phenomena underlying these imaging tools are going to be briefly analyzed in the following sections, in order to undestand how they can provide helpful information and the reasons why $Mn$ is an interesting tool.

[1] In other words it can be a particular pharmaceutical chosen accordingly to the target it has to reach or a molecule that has a pivotal role in some biological process , in order to obtain information about it

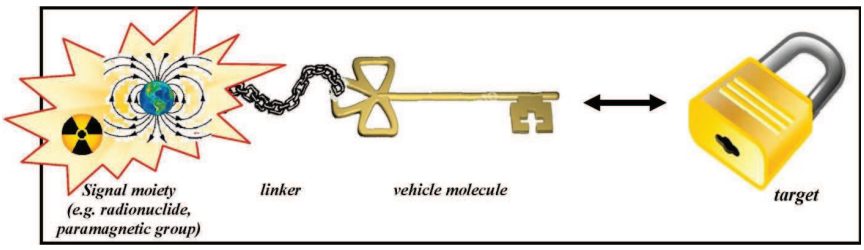


Figure 2.1: Radiopharmaceutical's schematic structure (picture taken from [6])

### 2.1.1 PET

PET imaging is based on the utilization of unstable isotopes of a nucleus that decay by emission of a positron ($\beta^+ decay$); once this nucleus is bound to a molecule in order to create radiopharmaceuticals it can be injected in the body. At this point, while decaying, the emitted positron will cover a length inside the cell proportional to it's energy (see previous definition of *Range*) and as soon as it is at rest in the laboratory frame it will annihilates with an electron producing two photons at $E_\gamma = 511\,keV$, same mass of an electron/positron. These photons will be produced at the same time and will travel in opposite directions due to quadrimomentum conservation and will be detected in coincidence[2] by a circular array of detector (usually scintillator) put around the patient's body. Once they get detected it is possible to localize their source along a straight line of coincidence (also called the line of response, or LOR) and to use these data for image reconsruction. Modern PET system can better localize the point of origin of the annihilation event and get a better image resolution with a method called Time of Flight technology using the simple kinematical relation (the speed of light and the time interval between the arrival of the two $\gamma$s is known) $D = c\Delta t/2$ [7] . In Table 2.1 there is a comparison

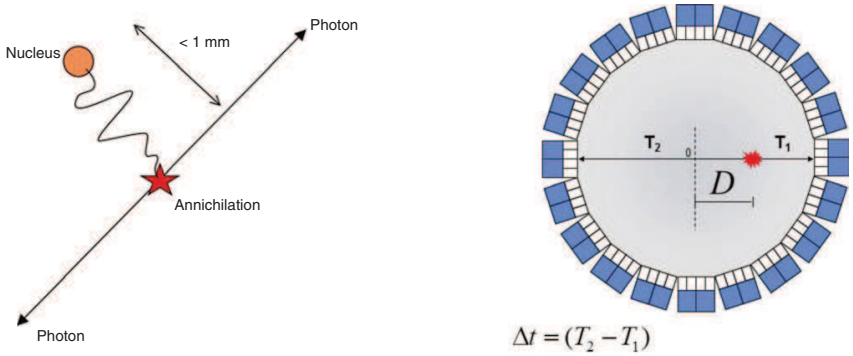


Figure 2.2: Annihilation of a positron with an electron (left) and its detection (right)

between $Mn$ isotopes and the most used radionuclide, $^{18}F$ which displays very competitve properties with respect to others. For example $^{51}Mn$ emits positron at very high energy and this made the

[2]Actually one should search for "true" coincidences since possible contaminations due to scatter events or random coincidences could occur generating a wrong image

spatial resolution very poor (few millimiters traveled before annihilation make hard to go back to the original position of the radiopharmaceutical) while $^{18}F$ and $^{52}Mn$ travel less than a millimiter.

Table 2.1: Comparison between $Mn$ isotopes and other studied radionuclides for PET (data taken from [8])

| Radionuclide | Half-life | *Endpoint* energy ($MeV$) | Intrinsic loss of resolution ($mm$) |
|---|---|---|---|
| $^{18}F$ | $1.83\,h$ | 0.635 | 0.7 |
| $^{51}Mn$ | $46.2\,min$ | 2.21 | 2.9 |
| $^{52}Mn$ | $5.59\,days$ | 0.575 | 0.63 |
| $^{52m}Mn$ | $21.1\,min$ | 2.63 | 3.5 |
| $^{64}Cu$ | $12.7\,h$ | 0.657 | 0.73 |
| $^{89}Zr$ | $3.27\,days$ | 0.897 | 1.0 |

The physical half-life is another important parameter to look at: $^{52}Mn$ has a quite long one so that it is possible to get various images acquired through PET even days after the initial administration [3]; this could be very useful if tracing molecules with long biological life (such as antibodies). Therefore, in this case, it should be used a radiopharmaceutical with a proper time of retention in organs in order not to expose the patient to very high doses, for example this is what happens with $MnCl_2$.

Very different scenarios for $^{18}F$ and $^{51}Mn$ that will stay in the organism much lesser time and are exploited to study fast processes (for example $[^{18}F]$[FDG] is used to detect cancer cells and exploits the fast glucose metabolism).

### 2.1.2 MRI

MRI imaging relies on a different physical mechanism that does not require radiation or unstable nuclei that is the coupling of a magnetic moment with a magnetic field. The human body is made of water ($H_2O$) and fat and this means that here is a lot of hydrogen in our body. Hydrogen is the simpliest atom of the periodic table, made by one proton and one electron: the proton is a particle that possesses an intrinsic angular momentum called spin and $s_p = \hbar/2$ (the proton is a 1/2 spin particle). The spin of a particle is a quantum phenomen that has no classical equivalent and it has been observed experimentally that it's value (along any axis of a frame) is always $\pm 1/2$[3] and that, until it is measured, it can have both value with equal probability. In other words, the proton does not have a value for its spin until it's measured and this lead to an important macroscopic consequence: the mean magnetic field produced by this layout of spins is null. The spin of proton is responsible for nuclear magnetic moment of the particle itself that, like any classical magnetic dipole, turns to align to any external magnetic field in order to minimize the energy of the system. In MRI this mechanism is exploited and the patient is exposed to an intense external magnetic field that gives rise to a magnetization field generated by coherent orientation of the nuclear magnetic moment of every proton, even though it is too small to be detected. That's why the technique of resonance is used: a mechanism that generate a RadioFrequency is applied to the target zone so that the amplitude of the oscillations of the spins[4] increases and the variation in time of this oscillating magnetization field is detectable from the instrumentation. [7]

This technique can be enhanced by the use of metals called *paramagnetic*: these materials' molecules show an intrinsic magnetic dipole that could aligns in the same direction of the external magnetic field increasing its intensity; therefore it's evident that they can be used to have better contrast in specific tissues where they have been absorbed making the image obtained more clear and sharp than what gained with standard technique.

[3] in unit of the reduced Planck constant $\hbar$

[4] if the spin is not perfectly aligned to the magnetic field it will start to precede around it, creating an oscillatory motion

## 2.2 $Mn$ application

We want to know at this point what are the common features of $^{51}Mn$ and $^{52}Mn$ and why they are so promising and inviting in the field of Nuclear Medicine for diagnostic purposes. The reason is that they show many improvement if used in MRI and PET with respect to other agents or radiopharmaceuticals and this means that they can easily can be exploited in the new and promising instrument that combines both the previously discussed techniques.

$Mn$ was chosen primarly for its fundamental role in human biological processes and for a possible combined MRI/PET that should have given a lot information in such applications like inestigation in neural tract tracing [12], diagnosis and staging of pancreatic cancer (detection of $\beta$-cells) and in general the need to follow stem cells' position, dynamic and survival. [11]

MRI does not require unstable nuclei so the discussion is the same for both the isotopes; usually this technique exploit the protons present in most of human tissue in order to perform clinical exams, even though paramagnetic metals could improve it giving way better results. The most used paramagnetic elements was gadolinium that shows very good properties but the search for now elements to be exploited has started when it was observed that $Gd$ induced a medical condition (in patients who alrady have renal problems) known as nephrogenic systemic fibrosis (NSF) [9], that is a very harmful side effect. Obviously this raised questions about its applicability in medical diagnosis using MRI and this is why there's been an increase in research of new paramagnetic elements that can be used as contrast agents.

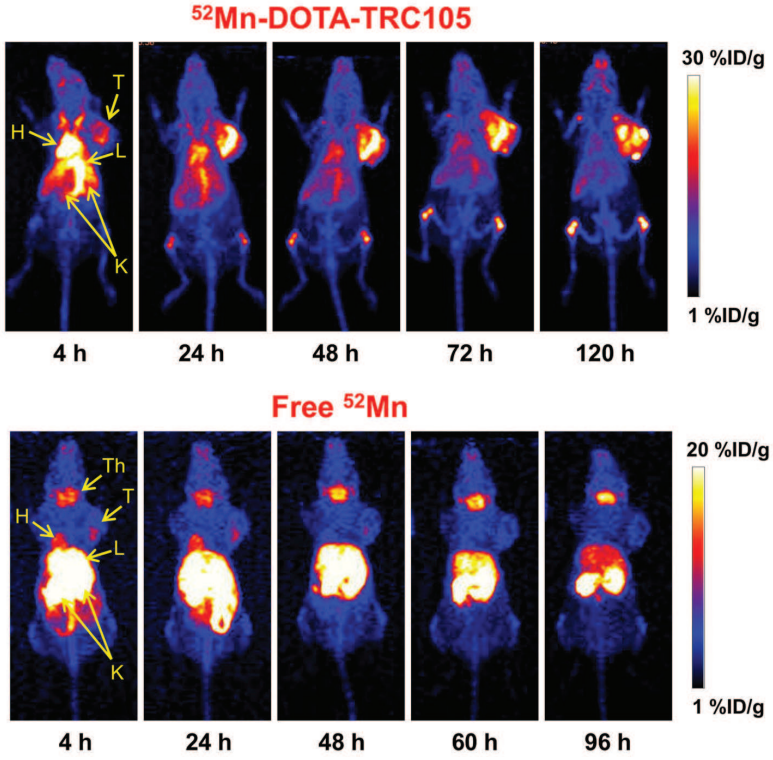


Figure 2.3: Differences in distributions between free ion $Mn$ and DOTA chelates
Note: H, Heart; L, Liver; K, Kidneys; T, Tumor; Th, Thyroid

The most popular form used is manganese as free ion ($MnCl_2$) and its relative technique is called MEMRI (Manganese-Enhanced MRI); indeed manganese shows very good paramagnetic properties when is oxidation number is 2 because of his *high spin*, id est his 5 unpaired electrons [10], that can easily couple with the external induced magnetic field. Even though has shown very good results in generating brighther signals [10] it has a quite heavy drawback: the ionic form of manganese is

extremely toxic [5] and adding this information to its long biological life it is clear that its application could be risky. This problem with free manganese seems to be avoided by using chelated manganese [9], where the metal is linked through coordinate bonds to some ligands (usually organic compounds). Basically the $Mn$ ions cannot move free in the organism because of the macromolecules it is bond to and several studies have made use of a molecule called DOTA (1,4,7,10 tetraazacyclododecane 1,4,7,10 tetraacetic acid) for its chelation stability with Mn(II) and for its widely spread utilization in radiochemistry. [12] A great difference between free manganese and DOTA chelates is evident even in their distribution as represented in Figure 2.3 where it is clear that the latter is well distributed in the target region (tumoral cells) instead of free $Mn$ that will execute its biological role (for example is an important nutrient in mammals feeding) and concentrate in other region (image acquired with a PET scan taken from [12]).

On the other hand, all these problems of administrated amount of manganese for MEMRI and its toxic effect are completely avoided for PET application since a lower dose can be injected (many orders of magnitude) while absolving its task as radiotracer and therefore being detectable [3]. Unstable nuclei used in radiopharmaceuticals that will be then exploited for PET imaging should have some basic requirements: low positron range (let's say less than a mm) in order to have a very good spatial resolution (for example in cases in which small structers need to be scanned); the radioactive nucleus should decay to a stable one and there should be no prominent emissions of high energy $\gamma$ during the de-excitation of the daughter nucleus (to avoid other decays and further radiations in both cases) [8].

As for the isotopes of interest, $^{52}Mn$'s long half-life could be a double-edged knife[6] while $^{51}Mn$'s half-life is suitable for just one PET scan (time of the order of $^{18}F$); on the contrary $^{52}Mn$ has a very good spatial resolution (positron emitted travels less than fluorine's one) while the very high energetic $^{51}Mn$'s positron ($> 2\,MeV$) makes very poor resoluted images. [4] [12]

[5] It has been observed that injected values above $10\,mg/kg$ of $MnCl_2/body\,mass$ (that are tipically administered in studies as bolus) are dangerous for the animal and may have long-term negative effects [3]

[6] Discussed previously, has both pros and cons: very usefull to acquire subsequent scans many days after the initial injection but this increases the level of radiation absorbed

# Chapter 3

# Dosimetric evaluation

We've seen that both isotopes of $Mn$ shown before could be useful tools for PET and MRI but it is also important to determine how much energy a radioactive nucleus transfers to the human body. A radiation dose analysis is fundamental for diagnostic application of radiopharmaceuticals but clearly this is not a measure that can be done directly, so it is necessary to develop methods to asses desired values in order to gain information about the energy irradiated by a radionuclide. This is the purpose of *dosimetry*, that despite its name (metry is related to experimental measures) concerns theoretical calculations and models (often it is referred to as *internal* dosimetry when dealing with radiations from inside the human body). A powerful tool in calculations of internal dose assessment (that will be used in this work, too) is the OLINDA[1]/EXM [16] code version 1 which contains decay data for more than 800 radionuclides and weighting factors (for both emitted radiations and organs) as defined by the ICRP (*International Commision on Radiological Protection*) 60[2] [14]; in detail, the job of OLINDA is to compute $DFs$ factors defined in 3.9 and, given the number of disintegrations $N$ that occurred in the source region, the equivalent dose $H_T$ of 3.10.

After having introduced some basic definitions of internal dosimetry, methods on how to compute these quantities will be presented as well as appropriate changes in data acquired on animal (whereas we are interested in human application). Afterwards all these tools will be used to perform a proper dosimetric evaluation on human beings with two different methods, based respectively on data acquired by Hernandez et al. [19] and by Graves et al. [4] on animal subjetcs using ionic form manganese.

All the informations about *dosimetry* in Nuclear Medicine have been taken from [13].

## 3.1 Basic concepts of dosimetry

First it is necessary to introduce a physical quantity that describes and quantify the radiation transferred to the absorber mean (the patient's body) and this is the *absorbed dose* defined as the energy absorbed per unit of mass:

$$D = \frac{d\varepsilon}{dm} \tag{3.1}$$

The absorbed dose has the dimension of energy/mass and in the SI its unit is the gray ($Gy$) and $1\,Gy = 1\,J/1\,kg$. Another important quantity is the *equivalent dose* that is defined as

$$H_{T,R} = w_R D_{T,R} \tag{3.2}$$

where $w_R$ is a weighting factor that takes in account the different possible damage dealt to the target depending on the type of incident radiation ($\gamma$, alpha, proton, neutron, etc.) and it is dimensionless and $D_{T,R}$ is the energy transferred by the radiation R to the tissue or organ T. This means that the

[1] *Organ Level INternal Dose Assessment*

[2] actually OLINDA code employs weigthing factors for human tissues that have been modified in ICRP 103 [17]

unit of equivalent dose should be the same of absorbed dose and to highlight that they are different quantities its unit is sievert ($Sv$) and values of $w_R$ are listed in Table 3.1.

Table 3.1: Weighting factors $w_R$ for different type of radiation as defined in ICRP 60 [14] (used in OLINDA v.1) and in ICRP 103

| Type of radiation | ICRP 60 | ICRP 103 |
|---|---|---|
| Photons (all energies) | 1 | 1 |
| Electrons and muons (all energies) | 1 | 1 |
| Neutrons | | |
| $< 10\,keV$ | 5 | |
| $10\,keV$ to $100\,keV$ | 10 | A continous curve as |
| $> 100\,keV$ to $2\,MeV$ | 20 | a function of neutron energy |
| $> 2\,MeV$ to $20\,MeV$ | 10 | |
| $> 20\,MeV$ | 5 | |
| Protons | 5 | 2 |
| Alpha particles, fission fragments, heavy nuclei | 20 | 20 |

One method to evaluate the term $D_{T,R}$ for internal dose assessment when a radioactive source is inside the target region is the following (that is its time derivative, yet):

$$\dot{D}_{T,R} = \frac{kA \sum_i y_i E_i \phi_i}{m} \tag{3.3}$$

where $k$ is just a numerical constant placed in order to have the dose expressed in the desired units (SI or not), $A$ is the activity of the radiation source defined as the number of disintegrations the occurs per unit of time $A = \frac{dN}{dt}$[3], $E_i$ is the energy of the emitted radiation, $y_i$ is the number of radiations with energy $E_i$ that occurs per nuclear reaction, $\phi_i$ is the fraction of emitted energy absorbed by the target and $m$ is the mass of the target. Actually we are interested in computing its time-integral, indeed the units of $\dot{D}$ (in SI units) are $Gy/s$ due to the presence of the activity and represents the *absorbed dose per unit of time*. To know the total energy transferred we should know how many disintegration occurs in the period of time in which the source is in the absorber medium and this is equivalent to compute the integral of activity over time, whatever the function $A(t)$, called time-activity curve, is. Obviously we need to make some assumptions on the form of this unknown functions: at first we could consider a case in which the activity decreases just by radioactive decay (exponential law) $A(t) = A_0 e^{-\lambda t}$ and the computation becomes trivial

$$\frac{\tilde{A}}{A_0} = \frac{1}{A_0} \int_0^\infty A(t)\, dt = \int_0^\infty e^{-\lambda t}\, dt = \frac{1}{\lambda} = \frac{t_{1/2}}{\ln 2} \tag{3.4}$$

$\tilde{A}$ is called *cumulated activity* and has just been divided for its initial amount[4] and this ratio is called *normalized cumulated activity*; in the last passage the relationship between decay constant and half-time was used to rewrite the result obtained as a function of a physical property of the radioactive nucleus. At this point by just replacing $A \to \tilde{A}/A_0$ and inserting all the decay informations required, the absorbed dose can be computed. It's important to note, though, that the integral just calculated has the dimension of a time and in order not to get confused about its meaning, it has the unit of $Bq\,h/Bq$.

However we can make a further assumption: usually the radiopharmaceuticals are excreted by the organims, i.e. they have another way to "decay" that is related to biological processes and the simplest (but that fits very well with experimental data) hypothesis is that it follows an exponential law, too. So, given the biological decay $X(t) = X_0 e^{-\lambda_b t}$ its integral is the same as what computed before

[3] $A$ is measured in Bq (becquerel) and $1\,Bq = 1\,disintegration/1\,s$

[4] so that the numerical value inserted in the absorbed dose formula does not depend on the number of administered activity

and considering the superpositions of these two decay mode (physical+biological) the effective decay constant is $\lambda = \lambda_p + \lambda_b$. It may happen in practice that the biological life of radiopharmaceutical is represented by a sum of exponential law (basically we are in the same assumptions stated before) in the form $X(t) = f_1 e^{-\lambda_1 t} + ... + f_n e^{-\lambda_n t}$ and assuming also the physical decay the cumulated activity is

$$\int_0^\infty X(t)\,dt = \int_0^\infty e^{-\lambda_p}(f_1 e^{-\lambda_1 t} + ... + f_n e^{-\lambda_n t})\,dt = \sum_i \frac{f_i}{\lambda_p + \lambda_i} = \frac{1}{\ln 2}\sum_i f_i T_i \tag{3.5}$$

it is easy to prove from $\lambda = \lambda_p + \lambda_b$ that

$$T = \frac{T_b T_p}{T_b + T_p} \tag{3.6}$$

Whatever the hypothesis we use to describe the system and do the calculations (physical decay or both physical and biological), we've derived a formula to calculate the absorbed dose in a very simple situation. In reality, the radiation emitted in a tissue could escape from it and contribute to the absorbed dose of another tissue so one just need to include all possible exchanges between tissues or organs. Before generalizing this formula it's necessary to mention that in the past years, many researchers have grouped many factors in the formula of absorbed dose above or changed a bit some definitions obtaining different equations that have the same meaning and lead to the same numerical results. The notation that is going to be used is the one of the RADAR[5] system that is

$$D = N \cdot DF \tag{3.7}$$

where $N$ is the number of disintegrations that occurs in the source region $S$ and

$$DF = \frac{k\sum_i y_i E_i w_i \phi_i}{m} \tag{3.8}$$

is the *dose factor* (note that the addition of the weighting factor just gives as a result of the previous calculation the *equivalent dose* and does not change the previous equations). By separating these two terms it is more clear how to perform the calculations since the term $N$ can be easily obtained from experimental data as the time-activity curve's integral while the *dose factor* $DF$ needs to be calculated starting from decay parameters and even Monte Carlo simulations in order to evaluate the terms $\phi_i$ (fraction of energy released by the radiation in the medium). One important parameter that needs to be evaluate in 3.8 is the mass of the organ that is being studied; this means that phantoms resembling the human body are necessary in order to simulate different cases. A phantom is a mathematical representation of the human body used to calculate Dose Factors. The OLINDA software has already implemented 10 different phantoms (male and female adult, newborn, 4 phantoms spanning from 1 to 15 years old and 3 phantoms for pregnant woman); the one used here is the adult male phantom (see Table 3.2) and was originally developed for the Medical Internal Radiation Dose Committee (MIRD) of the Society of Nuclear Medicine; it is an approximation of the human body based on simple geometrical shapes.

Now we can generalize to the case of target $T$ and multiple sources $S$ that is simply

$$DF_S = \frac{k\sum_i y_i E_i \phi_i(T \leftarrow S) w_i}{m_T} \tag{3.9}$$

and therefore, adding up all the contributions from various sources to the same target, the resulting *equivalent dose*

$$H_T = \sum_S N_S \cdot DF_S \tag{3.10}$$

By the way it's necessary to notice that the same equivalent dose to different organs or tissues may be more dangerous to some with respect to others. This is why the ICRP introduced another physical

[5] *RAdiation Dose Assessment Resource*, an electronic resource that was created on the internet at the beginning of this century in order to provide useful dose data worldwide

Table 3.2: Mass values of adult male phantom present in OLINDA v.1

| Tissue | Masses (g) |
|---|---|
| Adrenals | 16.3 |
| Brain | 1420 |
| Breasts | 351 |
| Gallbladder Walls | 10.5 |
| Small Intestine | 677 |
| Stomach Wall | 158 |
| ULI Wall | 220 |
| Heart Wall | 316 |
| Kidneys | 299 |
| Liver | 1910 |
| Lungs | 1000 |
| Muscles | 28000 |
| Ovaries | 8.7 |
| Pancreas | 94.3 |
| Red Marrow | 1120 |
| Osteogenic Cells | 120 |
| Skin | 3010 |
| Spleen | 183 |
| Testes | 3.91 |
| Thymus | 20.9 |
| Thyroid | 20.7 |
| Urinary Bladder Wall | 47.6 |
| Uterus | 79.0 |
| Total Body | 73700 |

quantity in order to consider these differences called *effective dose* [15] and it is defined, in a similiar way to what it has been done for *equivalent dose*, as

$$E = \sum_T H_T \cdot w_T \tag{3.11}$$

In this way the *"relative radiosensitivity of each organ for expressing fatal cancers or genetic defects"* [13] is taken in account and it *"represents the equivalent dose, which, if received uniformly by the whole body, would result in the same total risk as that actually incurred by a given actual nonuniform irradiation"* [13]. The effective dose is used to compare the different doses that the same subject has absorbed from different sources and it can be added to doses coming from other radiations in order to quantify the total dose (for example when assessing the radiation intake after different medical exams). Values of $w_T$ used by OLINDA are listed in Table 3.3 and are taken from [14], even though new factors are available [17].

## 3.2 Dose assessment calculations

In order to perform dosimetry calculations is fundamental to know (given the radionuclide to study) the disintegrations occured in the organs where the radiopharmaceuticals has accumulated. To do this one needs to understand how it spreads all over the body and which organs have high concentration of it, namely the biodistribution of the pharmaceutical. In this work it is going to be evaluated the dose of $MnCl_2$, that once injected it separates into $Mn^{2+}$ and $Cl^-$, thus the biodistribution of manganese ions is needed.

There aren't many researches in literature with good biodistribution data (measurements acquired in

Table 3.3: Weighting factors for different organs as defined in ICRP 60 [14] and in ICRP 103 [17]

| Organ | ICRP 60 | ICRP 103 |
|---|---|---|
| Bone surfaces | 0.01 | 0.01 |
| Bladder | 0.05 | 0.04 |
| Brain | // | 0.01 |
| Breast | 0.05 | 0.12 |
| Colon | 0.12 | 0.12 |
| Gonads | 0.20 | 0.08 |
| Liver | 0.05 | 0.04 |
| Lungs | 0.12 | 0.12 |
| Oesophagus | 0.05 | 0.04 |
| Red bone marrow | 0.12 | 0.12 |
| Salivary Gland | // | 0.04 |
| Skin | 0.01 | 0.01 |
| Stomach | 0.12 | 0.12 |
| Thyroid | 0.05 | 0.04 |
| Remainder | 0.05 | 0.12 |

Table 3.4: Biodistribution of $^{52}Mn$ in various organs

All the values are in units of $\%ID$ (percentage of injected dose) and decay corrected, i.e. they represents just biological elimination; S Gland data has not been used for dosimentric evaluations since it is not present in OLINDA v.1

| Time (h) | Heart | Liver | Kidneys | Muscle | Pancreas | Salivary Gland |
|---|---|---|---|---|---|---|
| 1 | $7.50 \pm 0.61$ | $11.63 \pm 1.12$ | $18.30 \pm 0.53$ | $1.37 \pm 0.12$ | $18.30 \pm 1.71$ | $8.20 \pm 0.92$ |
| 3 | $6.70 \pm 0.62$ | $12.00 \pm 1.41$ | $18.57 \pm 1.42$ | $1.37 \pm 0.06$ | $18.23 \pm 2.21$ | $9.00 \pm 1.35$ |
| 12 | $4.30 \pm 0.61$ | $12.50 \pm 0.69$ | $17.47 \pm 0.21$ | $1.27 \pm 0.15$ | $17.43 \pm 0.87$ | $9.87 \pm 0.49$ |
| 24 | $3.33 \pm 0.42$ | $11.20 \pm 0.72$ | $16.33 \pm 0.72$ | $1.17 \pm 0.12$ | $17.23 \pm 0.40$ | $9.60 \pm 0.30$ |
| 72 | $2.83 \pm 0.21$ | $6.90 \pm 0.46$ | $11.83 \pm 0.45$ | $0.96 \pm 0.15$ | $15.70 \pm 1.59$ | $10.17 \pm 0.37$ |
| 120 | $2.57 \pm 0.15$ | $5.30 \pm 0.10$ | $9.27 \pm 0.25$ | $0.93 \pm 0.06$ | $13.03 \pm 1.56$ | $11.20 \pm 0.85$ |
| 168 | $2.47 \pm 0.06$ | $3.83 \pm 0.29$ | $7.00 \pm 0.87$ | $0.73 \pm 0.07$ | $10.63 \pm 1.17$ | $10.77 \pm 0.71$ |
| 216 | $2.30 \pm 0.10$ | $2.93 \pm 0.15$ | $5.57 \pm 0.84$ | $0.64 \pm 0.05$ | $8.07 \pm 0.90$ | $9.63 \pm 0.32$ |
| 264 | $2.07 \pm 0.15$ | $2.50 \pm 0.10$ | $4.57 \pm 0.61$ | $0.66 \pm 0.02$ | $6.43 \pm 0.95$ | $9.37 \pm 0.55$ |
| 312 | $1.93 \pm 0.06$ | $2.20 \pm 0.10$ | $4.03 \pm 0.31$ | $0.66 \pm 0.05$ | $5.90 \pm 1.20$ | $8.90 \pm 0.26$ |

limited intervals of time with respect to radionuclide's half-life or very few samples); the best data that have been found for this work has been recovered from Hernandez et al. [19] and Graves et al. [4] and since these articles starts from different hypothesis and provides different data, different paths will be followed for the internal dose assessment.

The purpose of the former is to show that $^{52}Mn$ can be used for PET imaging of $\beta - cells$ instead of its use in MRI (due to its cytotoxic effect) and although $Mn$ uptakes for some organs are reported (see Table 3.4) no dosimetric evaluations have been done. All the values reported represent the activity measured in a selected target region *in vivo* on animal via PET scans: this method affects the reliability of the measures done because of the difficulty and uncertainty in selecting the region of interest from which acquire $^{52}Mn$ activity, especially on little areas. Moreover, it is important noticing that the previous data were acquired from animals: dosimetric evaluations can be performed just by using them or applying some changes to make them more suitable for human application. One of them is the mass extrapolation: basically it consists in rescaling the data measured from mice to humans by multiplying for a factor that takes into account the different percentage over the total body mass of single organs

$$\left(\frac{\%}{organ}\right)_{human} = \left[\left(\frac{\%}{g_{organ}}\right)\cdot(kg_{TB})\right]_{animal}\cdot\left(\frac{g_{organ}}{kg_{TB}}\right)_{human} \tag{3.12}$$

The first term represents the percentage of total activity administered that would accumulate in the human organ , $\left(\frac{\%}{g_{organ}}\right)_{animal}$ is the activity uptake in a particular organ divided by the mass of the animal's organ and the remaining terms are the mass of organs and total body of animal and human. In the Hernandez's experiment, the activity was measured using PET so the raw data are acquired in the SUV unit (*Standardized Uptake Value*) defined as $SUV = \left(\frac{\%}{g_{organ}}\right)\cdot(kg_{TB})$; in this unit the previous formula becomes

$$\left(\frac{\%}{organ}\right)_{human} = SUV_{animal}\cdot\left(\frac{g_{organ}}{kg_{TB}}\right)_{human} \tag{3.13}$$

From 3.13 it is possible to get the mass of the mice used in the experiment since Hernandez et al. reports data both in SUV unit and $\%ID$ and so

$$\frac{SUV}{\%ID/g} = mass_{TB} \approx 28g \tag{3.14}$$

Another possible correction to animal data that can be done is time extrapolation: basically it consists in changing the istant of time at which the uptake was measured based on the different metabolism of mice and humans and a simple empirical parametrization is given in [13]

$$t_{human} = t_{animal}\left[\frac{m_h}{m_a}\right]^{1/4} \tag{3.15}$$

Now it is possible calculating the effective dose for $^{52}Mn$ starting from its biodistribution in Table 3.4. The organs taken into account (for which are reported significant uptake value) are liver, pancreas, kidneys, heart and muscle; salivary glands' biodistribution is left out because there is not the possibility to insert its disintegrations' value in OLINDA v.1. All the data have been extrapolated to human (with only mass correction and then with both mass and time corrections) and in order to get information about the area underlying the points, the plot has been fitted with a sum of three exponential[6] decay $f(t) = \sum_{i=1}^{3} f_i e^{-\lambda_i t}$ that represent respectively the uptake,retention and elimination of the radiopharmaceutical in the organ selected. The result of the fits are showed in Figure 3.1 and the area of the fit function has been computed according to 3.5 because data are decay corrected and therefore the physical decay constant needs to be added. The values obtained by integrating the previous distributions were then put in the OLINDA/EXM software together with the remaining activity that it is accumulated in the rest of the body, whose distribution is unknown. To do so, there's the possibility in OLINDA to insert the value of the remaining activity so that it will be spread over all other tissues in proportion to their mass. The remaining activity was calculated by assuming both physical and biological decay (in order to consider all form of elimination of $Mn$ from the body and get more reliable results). Biological decay of $Mn$ has been studied in [18] and it was found that it can be described as the sum of two exponential decay that has a *slow* component of half-life equals to 39 days (about 70% of $Mn$ is eliminated this way) and a *fast* component (for the remaining fraction) of half life equals to 4 days. In the end, the total activity is

$$\frac{A_{tot}}{A_0} = \int_0^\infty e^{-\lambda_p}(0.7^{-\lambda_{slow}t} + 0.3^{-\lambda_{fast}t})\,dt = \frac{0.7}{\lambda_p + \lambda_{slow}} + \frac{0.3}{\lambda_p + \lambda_{fast}} \tag{3.16}$$

[6]Exponentials are heavily used in this context: they are easy to integrate and they describes very well experimental data

and the remaining activity is simply calculated by subtracting the results of the area derived from the fitted curves. All these calculations can be extended to $^{51}Mn$ either, in fact it's necessary to just change the physical decay constant in the integrals above (both in 3.5 for the area under the curves and in 3.16 for the assessment of the remaining activity) since biodistribution is the same for different isotopes of an element.

The article of Graves S. A. et al. [4] deals with production, characterization by *in vivo* behavior and preliminary dosimetric predictions of $^{51}Mn$ and actually, in this case, there aren't any biodistribution data reported and thus disintegrations in source organs have already been computed by the authors (see Table 3.5, central column). Even this time, the experiment has been conducted on animals but this time no mass/time extrapolation or other methods have been used by Graves et al. [4]; also, since the experiment involved $^{51}Mn$, uptake values in animals' organs have been acquired for far less time (up to $\sim 90\,min$) than what has been done for $^{52}Mn$ in [19] ($13days$). As a consequence, Graves et al. have considered only physical elimination (i.e. radioactive decay) because of the relative quite long biological elimination path. Thus, by multiplying $^{51}Mn$ disintegrations for the ratio of the two $Mn$ isotopes' half-lives it is possible to rescale the given data and perform a dosimetric evaluation for $^{52}Mn$ even with this data (Table 3.5, right column).

Table 3.5: Numbers of disintegrations per unity of activity administered

All the data reported here are in units of MBq-h/MBq and the ones in central column are taken from [4]

| Tissue | Numbers of $^{51}Mn$ disintegrations | Numbers of $^{52}Mn$ disintegrations |
|---|---|---|
| Adrenals | 0 | 0 |
| Brain | 4.43E-03 | 0.77 |
| Breasts | 0 | 0 |
| Gallbladder Contents | 0 | 0 |
| LLI | 0 | 0 |
| Small Intestine | 0 | 0 |
| Stomach | 0 | 0 |
| ULI | 6.42E-03 | 1.12 |
| Heart Contents | 0 | 0 |
| Heart Wall | 2.37E-02 | 4.13 |
| Kidneys | 6.91E-02 | 12.0 |
| Liver | 6.30E-02 | 11.0 |
| Lungs | 1.68E-02 | 2.93 |
| Muscles | 2.18E-03 | 0.38 |
| Ovaries | 0 | 0 |
| Pancreas | 4.11E-02 | 7.16 |
| Red Marrow | 0 | 0 |
| Cortical Bone | 8.40E-04 | 0.15 |
| Trabecular Bone | 0 | 0 |
| Spleen | 9.16E-03 | 1.60 |
| Testes | 0 | 0 |
| Thymus | 0 | 0 |
| Thyroid | 0 | 0 |
| Urinary Bladder Contents | 0 | 0 |
| Uterus/Uterine Wall | 0 | 0 |
| Total Body | 8.70E-01 | 152 |

## 3.3 Results

As for the first method described, based on Hernandez's experiment, the data computed for $^{51}Mn$ and $^{52}Mn$ have been inserted into OLINDA using adult male phantomand the relative effective doses are listed in Table 3.6.

Table 3.6: Effective doses calculated for $^{51}Mn$ and $^{52}Mn$ with both the methods; all values are reported in $mSv/MBq$

| Isotope | Herndandez's data | | Graves' data |
|---|---|---|---|
| | Real Time | Corrected Time | |
| $^{51}Mn$ | $1.12 \cdot 10^{-2}$ | $1.13 \cdot 10^{-2}$ | $1.24 \cdot 10^{-2}$ |
| $^{52}Mn$ | 1.61 | 1.62 | 2.38 |

There is nearly no difference between time corrected and real time doses, so in this case the two methods give essentially the same result. With the second method, so starting from Graves et al. data, the effective dose of an adult male phantom for $^{52}Mn$ is $2.38\,mSv/MBq$ whereas $^{51}Mn$'s one ( $1.24 \cdot 10^{-2}\,mSv/MBq$) calculated with OLINDA gives the same value the authors have found[7]. By making a comparison between the effective dose obtained for $^{51}Mn$ and $^{52}Mn$ it is evident that the second method produces higher values and this could be due to many factors: for example, Graves et al. did not make use of mass extrapolation on animal data and have supposed only physical decay without any biological elimination path that would have speed up its clearence from the body. On the contrary, calculations based on biodistribution data acquired for longer period (the order of three times the radionuclide's half-life) should be preferable in order to take into account even biological processes and have more reliable evaluations.

In Table 3.7 a comparison is presented between the dose absorbed of $^{52}Mn$ by each target organ for the two evaluations performed: nearly all the values computed starting from Graves et al. data are higher than those obtained from Hernandez et al. except for brain. Considering that $Mn$ plays important biological roles in this organ and that this could lead to longer retention in them [12], this underestimate could be due to the very short time the $Mn$ biodistribution was measured by Graves et al. with respect to Hernandez et al.

Just to have an idea of the order of magnitude of effective dose administered by radiopharmaceuticals that are already being used in clinical practice, we could consider $[^{18}F]$[FDG] that is a $^{18}F$ -based radiopharmaceutical which effective dose is $0.019\,mSv/MBq$ [14]. As expected, $^{52}Mn$ transfers a quite higher dose due to his long half-life and emissions of high energy photons, making it ill-suited for clinical purpose in free ion form.

The only reference value found in literature, in order to make a comparison with the ones obtained in these calculations, for $^{52}Mn$ is in [8] and it is $0.924\,mSv/MBq$ that howewer has been derived assuming very simplistic hypothesis: a complete uniform distribution in man and a biological elimination time of $T_b = 100h$.

[7] actually in [4] it is computed the *effective dose equivalent* that is based on old ICRP 30 weigthing factor [15] while in the table is reported the *effective dose* that is based on ICRP 60 [14] factors

Table 3.7: Comparison of doses absorbed of $^{52}Mn$ by target organs computed with OLINDA v.1

All values are in unit of $mSv/MBq$ ; note that all values based on Graves et al. are higher than their counterparts obtained from Hernandez's biodistribution data except for brain

| Tissue | First method (Hernandez's data) | Second method (Graves' data) |
|---|---|---|
| Adrenals | 1.95 | 3.64 |
| Brain | 1.42 | 0.79 |
| Breasts | 1.18 | 1.77 |
| Gallbladder Walls | 2.14 | 3.49 |
| LLI Wall | 1.74 | 2.41 |
| Small Intestine | 1.96 | 2.97 |
| Stomach Wall | 1.79 | 3.35 |
| ULI Wall | 1.93 | 3.05 |
| Heart Wall | 1.78 | 4.25 |
| Kidneys | 2.42 | 9.13 |
| Liver | 2.49 | 3.62 |
| Lungs | 1.44 | 2.08 |
| Muscles | 1.26 | 1.72 |
| Ovaries | 1.79 | 2.50 |
| Pancreas | 2.78 | 13.4 |
| Red Marrow | 1.50 | 2.00 |
| Osteogenic Cells | 1.81 | 2.20 |
| Skin | 0.92 | 1.23 |
| Spleen | 1.75 | 4.48 |
| Testes | 1.29 | 1.72 |
| Thymus | 1.44 | 2.12 |
| Thyroid | 1.38 | 1.73 |
| Urinary Bladder Wall | 1.67 | 2.29 |
| Uterus | 1.83 | 2.59 |
| Total Body | 1.38 | 1.92 |

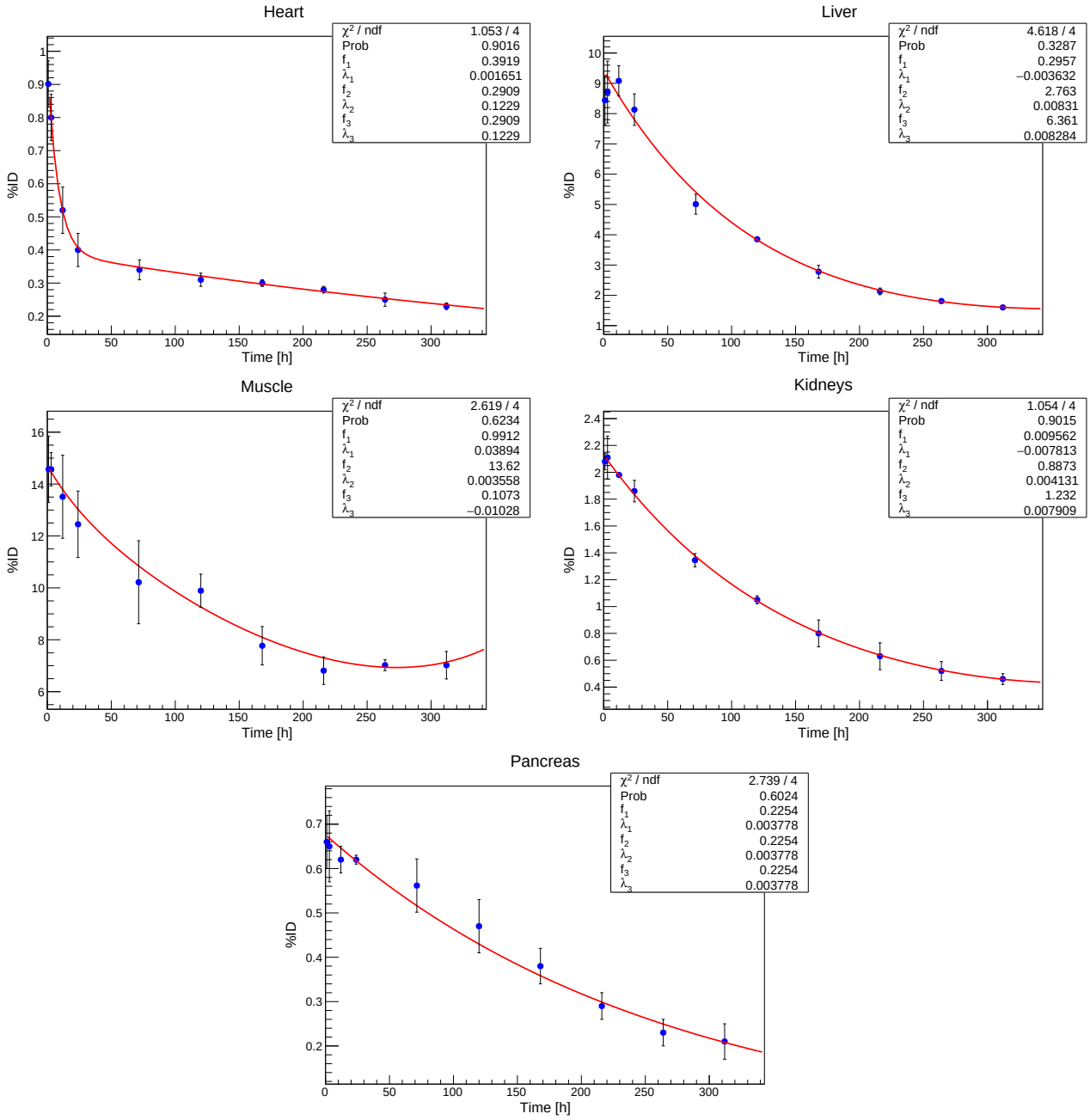


Figure 3.1: Time-activity curves have been calculated and plotted for organs displaying relatively high uptake

# Chapter 4

# Conclusions

MultiModal Imaging is a new tool in Nuclear Medicine that allows combining images with different diagnostic contents. In order to do this it is necessary to find a radionuclide that could show both good positron-emitting nuclear properties similar to $^{18}F$ and high paramagnetic properties: a possible isotope that satisfies these conditions is $^{52}Mn$. Various experiment have been carried out in order to study its possible application, e.g. the METRICS experiment at the INFN Laboratori Nazionali di Legnaro that aims at studying various aspects of the production of this radionuclide (possible contaminants, alterative production routes, etc.). Therefore the goal of this work is to perform a dosimetric assessment of the dose transferred to the human body by $^{52}Mn$-based radiopharmaceuticals. Data used to perform the calculations have been taken from Hernandez et al. [19], that reports $Mn$ biodistribution up to 13 days post injection of $MnCl_2$, and from Graves et al. [4], that on the other hand reports only disintegrations occured in source organs. These articles were chosen because have enough measures to perform dose calculations even though present many critical issues: biodistribution data taken from Hernandez et al. are obtained measuring the activity *in vivo* with PET scans and this could lead to problems due to the difficulty in selecting small region (overlapping); *ex vivo* measurements of the desired organ would be preferable and much more accurate than those reported. Instead, Graves et al. acquired data on $^{51}Mn$ measurements ($t_{1/2} = 46.2\,min$) and since it has a quite shorter half-life than the time requested for biological elimination, only radioactive decay was assumed as elimination path; furthemore, altough activity was measured on mice, no mass extrapolation correction for human application has been done.

Subsequently internal dose calculations have been done and, although the assements based on the two sets of data are a bit different different for the reasons showed before, $^{52}Mn$ shows very high doses (for example quite higher than [$^{18}F$][FDG]) as expected because of its long physical half-life combined with long retention in organs. The latter contribution is due to $Mn$ ions long biological half-life fromed after the $MnCl_2$ dissociated itself: of course better radiopharmaceutical should employs chelates in order to prevent $Mn$ ions formation and speeding up its elimination. Actually, no dosimetric evaluations have been found in literature about the effective dose of $^{52}Mn$ (except [8] that yet uses too simplistic assumptions) so the results presented here should be considered as just a first step before successive and more complete $^{52}Mn$ studies (for example involving better radiopharmaceutical in order to avoid $Mn^{2+}$ formation or longer acquisition time for biodistribution measurements).

# Bibliography


[1] Kakavand T. et al., *Cyclotron production of* $^{52}Mn$ *and Monte Carlo benchmarking*, in "Journal of Radioanalytical and Nuclear Chemistry", n. 304, 2015, 669-674

[2] Kopka K., *Pharmaceuticals—Special Issue on Radiopharmaceutical Chemistry between Imaging and Endoradiotherapy*, in "Pharmaceuticals" 2014, 7, 839–849

[3] Topping G.J., *Manganese-52 positron emission tomoghraphy tracer characterization and initial results in phantoms and* in vivo, in "Medical Physics" Vol. 40, No. 4, April 2013

[4] Graves S. A. et al., *Preparation and* in vivo *characterization of* $^{51}MnCl_2$ *as PET tracer of* $Ca^{2+}$ *channel-mediated transport* , in "Scientific Report" 7, Article number: 3033 (2017)

[5] Buchholz M. et al., *Cross-section measurements for the formation of manganese-52 and its isolation with a non-hazardous eluent*, in "Radiochimica Acta", 101, 2013, 491-499

[6] Mitterhauser M., Wadsak W., *Imaging Biomarkers or Biomarker Imaging?*, in "Pharmaceuticals" 2014, 7, 765–778

[7] Gareffa G., Hagberg G., Indovina L., *Physics of Hybrid Imaging*, in "PET-CT and PET-MRI in Neurology" 2016, 3-11

[8] Pagani M., Stone-Elander S., Larsson S. A., *Alternative positron emission tomography with non-conventional positron emitters: effects of their physical properties on image quality and potential clinical applications*, in "European Journal of Nuclear Medicine" Vol.24, No. 10, October 1997

[9] Pan D. et al., *Manganese-based MRI contrast agents: past, present and future*, in "Tetrahedron" 2011, 67(44), 8431-8444

[10] Wooten A. L. et al., *Biodistribution and PET Imaging of pharmacokinetics of manganese in mice using Manganese-52*, in "Plos One" 2017, 12(3)

[11] Lewis C. M. et al., $^{52}Mn$ *production for PET/MRI tracking of human stem cells expressing divalent metal transporter 1 (DMT1)*, in "Theranostics" 2015, 5(3), 227-239

[12] Graves S. A. et al., *Novel preparation methods of* $^{52}Mn$ *for ImmunoPET Imaging* , in "Bioconjugated Chemistry" 2015, 26(10), 2118-2124

[13] Stabin M. G., *Fundamentals of Nuclear Medicine Dosimetry*, Springer, 2006

[14] International Commision on Radiological Protection. *1990 Recommendations of the International Commission on Radiological Protection.* New York, NY: Pergamon Press; 1991. ICRP publication 60.

[15] International Commission on Radiological Protection. *Limits for Intakes of Radionuclides by Workers.* ICRP Publication 30. Pergamon Press, New York, 1979.

[16] Stabin M. G., *OLINDA/EXM: The second-generation personal computer software for internal dose assessment in Nuclear Medicine*, in "Journal of Nuclear Medicine" 2005, Vol.46, 1023-1027

[17] International Commision on Radiological Protection. *The 2007 Reccomendations of the International Commission on Radiological Protection*

[18] Mahoney J. P., Small W. J., *The biological half-life of radiomanganese in man and factors which affect this half-life*, in "The Journal of Clinical Investigation" 1968, Vol.47, 643-653

[19] Hernandez R. et al., *Radiomanganese PET detects changes in functional $\beta$-cell mass in mouse models of diabates*, in "Diabetes" 2017, Vol.66, 2163-2174